The kinetics of clustering in Al-Mg-Si alloys studied by Monte Carlo simulation

Zeqin Liang[a], Cynthia Sin Ting Chang[b], Christian Abromeit[a], John Banhart[a,b] and Jürgen Hirsch[c]

[a] Helmholtz-Zentrum Berlin für Material and Energy, Institute of Applied Materials, Berlin, Germany
[b] Technische Universität Berlin, Institute of Materials Science and Technology, Berlin, Germany
[c] Hydro Aluminium Deutschland GmbH, Bonn, Germany

Abstract

The kinetics of clustering in Al-Mg-Si alloy is studied by Kinetic Monte Carlo (KMC) simulations. The simulations take into account the probability of vacancy jumping to nearest neighbour sites. This probability is calculated by considering both the activation energies for single vacancy migration and the difference of interaction energies before and after jumping. The simulations show that clustering in Al-Mg-Si is fast and takes place in three stages. In the initial stage, dimers, trimer and small co-clusters form. The number density of such clusters increases rapidly and solute atoms aggregate to those clusters until a maximum density value is reached after 2 min. In the second stage from 2 min to around 100 min, a decrease of the number density of small clusters accompanied by an increase of the fraction of solute contained in all the clusters can be observed. Finally, coarsening of some of the clusters by coalescence was found, hence further reducing the cluster number density, while the amount of solute atoms in the clusters remains constant. We discuss how robust the results are with respect to changes of the input parameters.

Keywords: Kinetics, Clustering, Al-Mg-Si alloy, Kinetic Monte Carlo Simulation

1. Introduction

Alloys based on the Al-Mg-Si system are widely used because they can be artificially aged to medium strength whilst having good mechanical properties, good formability, weldability and corrosion resistance. [1] 'Room temperature' storage of these alloys, i.e. natural ageing (NA) at ≈20°C, between solution heat treatment and artificial ageing (AA) often has a negative effect on AA and cannot be avoided in the industrial process chain. This 'negative effect' is thought to be caused by the formation of clusters during NA [2] and it kinetics and mechanism are not yet fully understood. Clustering is a fast reaction and microscopic techniques fail to track the earliest stages due to unwanted ageing already during sample preparation[3] so that they are useful only for samples aged for a long time or at elevated temperatures [4,5,6]. Some indirect methods such as Positron Annihilation Lifetime Spectrum (PALS), in-situ resistivity measurement or Differential Scanning Calorimetry (DSC) can track clustering kinetics already in very early stages, but the results are difficult to analyse and interpret [7].

Simulation has proved to be useful for understanding reactions on the atomic scale. Recently, a realistic diffusion model based on vacancy migration has been incorporated into Kinetic Monte Carlo (KMC) modelling [8]. This approach can provide details on the kinetics of precipitation, including nucleation [9], vacancy trapping, diffusion and stabilization of small clusters [10,11,12]. Clustering during NA in Al-Mg-Si alloys is a low-temperature reaction driven by diffusion and we use KMC simulation to understand its kinetics. The simulation is based on the diffusion of a single vacancy and by considering both diffusion activation and interaction energies.

2. Simulation setup and parameters

Experiments have shown that the kinetics of clustering at 'room temperature' in Al-Mg-Si alloys is governed by the interaction of the quenched-in vacancies and solutes [7]. At this low temperature, clusters should not modify the crystal structure of the base alloy, i.e. the solute atoms belonging to a cluster are still located on positions of the fcc aluminium lattice and the lattice constant is only marginally changed. The size of the simulation box is 25×25×25 unit cell (62500 atoms) and periodic boundary conditions are applied in all the directions. In order to simplify the model, only a single vacancy is generated, which is conserved throughout the simulation. The vacancy is thermally activated and can jump to nearest neighbour (NNB) sites. The jump frequency of the vacancy towards each of its 12 NNBs is

$$w_i = v_i \exp\left(-\frac{E_i^{act}}{k_B T}\right), \qquad (i = 1,2,3 \ldots 12), \tag{1}$$

where v_i is the jump attempt frequency, E_i^{act} is the activation energy, k_B is Boltzmann's constant and T the temperature. One part of E_i^{act} is the migration energy of the vacancy into a site i (i=Al, Mg, Si) which can be determined by using the theoretical diffusion activation energy E_i^d and subtracting from this the formation energy of the vacancy E_V^f, both given in Table 1 (strictly speaking enthalpy, but here p and V are constant). The vacancy is assumed to have formed during quenching and is preserved after. E_i^{act} further contains the difference of the interaction energies of the vacancy with its nearest neighbourhood before and after the vacancy jumps. Therefore, the activation energy E_i^{act} required for the vacancy to move from its initial position j to the atom position i of its NNB atom i is expressed as,

$$E_i^{act} = E_i^d - E_V^f - \left(\sum_{k\in NNB_j} \varepsilon_{kV_{(j)}} + \sum_{k\in NNB_i} \varepsilon_{ki_{(i)}}\right) + \left(\sum_{k\in NNB_i} \varepsilon_{kV_{(i)}} + \sum_{k\in NNB_j} \varepsilon_{ki_{(j)}}\right) \tag{2}$$

Eq. (2) is an approximation, since we sum up pair interaction energies and therefore neglect

any interaction between such pairs. NNB_j denotes all the nearest neighbours of site j. ε_{kV} and ε_{ki} are the interaction energies of a vacancy or atom with their NNB. The published values [13,14,15] of v_i, E_i^d, E_V^f, ε_{kV} and ε_{ki} are listed in Tables 1 and 2 and serve as input parameters for our calculation. It should be mentioned that the interaction energies are calculated by subtracting pairs of reference configurations. This choice implies that $\varepsilon_{\text{Al-Al}}$, $\varepsilon_{\text{Al-V}}$, $\varepsilon_{\text{Al-Si}}$ and $\varepsilon_{\text{Al-Mg}}$ are zero [16].

A Monte Carlo Step (MCS) number can be converted to a physical time *t* by the following equation.

$$t = \frac{1}{NC_V \sum_{i=1}^{12} w_i}, \tag{3}$$

where C_V is vacancy concentration and N is the number of atoms in the simulated box. C_V is calculated by

$$C_V = \exp\left(-\frac{G_V^F}{k_B T}\right) \quad , \tag{4}$$

where G_V^F is the Gibbs free energy of formation. Since $G_V^F = \mathrm{H_V^F} - \mathrm{TS_V^F}$, by taking $\mathrm{H_V^F}$ = 0.67 eV and $\mathrm{S_V^F} = 0.7k_B$, [17,18] a value $C_V = 1.41\times10^{-4}$ can be obtained and is applied for our simulation. The NA temperature is 293.15 K and the simulated material is Al-0.67Mg-0.77Si (at.%) which corresponds to alloy 6-8(F) of previous experimental work [3,19]. 10 simulation runs are performed and averaged.

3. Results

We define that a cluster is any concentration of 2 or more neighbouring solute atoms. Figure 1 shows 3D mappings of Mg and Si atoms in clusters as obtained by KMC simulation for different selected times and as visualized using the software `Vesta`[20]. At the initial stage

before the simulation has started, dimers and trimers exist already in the computer-generated random distribution, see Fig.1a. After a short period of time, the number density of clusters visibly increases. However, the size of the clusters still remains small, as shown in Fig.1b. The clusters are still mostly dimers and trimers, although some solute chains can also be observed. With progressing NA, see Fig.1c, solute chains with an even larger number of solutes and clusters having more than 10 solute atoms are observed. After 100 min of NA, some of the clusters grow to more than 30 solutes, as shown in Fig.1d. After this, some big clusters coarsen and ordering within clusters is observed as displayed in Fig.1e.

The evolution of cluster number density and the fraction of solute contained in clusters with respect to the total number of solute atoms in the alloy is given in Fig. 2. For the first 2 min of NA, the number density and the percentage of solutes in the cluster both increase. After 2 min of NA, the number density of clusters starts to decrease, but the fraction of solutes still increases, indicating that some clusters grow by coalescence with other clusters, while some solute from the matrix is still added to the clusters. After 100 min of NA, the fraction of solute reaches a maximum value of ≈73% and becomes saturated after. The number density of clusters continues to decrease, indicating that in this stage pure coarsening takes place and no more solute atoms are added to the clusters from the matrix.

Size distributions of the clusters corresponding to the same times selected for Fig.1 are given in Fig. 3. The size distribution function of the clusters is defined as

$$f(x) = \frac{N_x x}{a}, \tag{5}$$

where N_x is the number of clusters containing x solute atoms and a is the total number of solute atoms in the simulation box. By this definition, $\sum_{x=2}^{\infty} f(x)$ equals the fraction of solutes

in all clusters as given in Fig. 2.

It can be seen from Figs. 3a and 3b that from the initial stage to 1 min of NA, the largest occurring cluster increases from 3 (trimers) to 15. On the other hand, the numbers of dimers and trimers increase from 14% to 21% and from 1.8% to 11% respectively. This means that in this stage rapid solute addition to clusters occurs and these grow continuously. Clusters containing ~25 solute atoms appear after 10 min of NA. After this, the contribution of dimers slightly decreases whereas that of trimers still increases, see Fig. 3c. After NA for 100 min, see Fig. 3d, clusters with more than 50 atoms start to appear while the contribution of clusters with less than 4 solutes decreases. The distribution profile after 1000 min of NA in Fig. 3e shows that 2 size distributions have appeared, forming a bimodal distribution: One located at $2<x<30$, the other at $30<x<65$. There is no significant change of the frequency distribution of clusters with less than 20 solutes, while the number of clusters with more than 35 solute atoms has increased sharply, which again indicates that coarsening of clusters occurs from 100 min to 1000 min.

4. Discussion

Analysis of the initially random distribution shows that dimers and trimers already exist in the initial stage, see Fig. 1a. The higher the solute concentration, the higher the probability will be that two solutes are found on neighbouring lattice sites. The probabilities P_2 and P_3 of the occurrence of such statistical dimers or trimers, resp., in a binary system can be calculated [21]

$$P_2 = 12pq^{18}, \tag{6}$$

$$P_3 = p^2(3q^{21} + 18q^{22} + 39q^{23} + 90q^{24}), \tag{7}$$

where p is the probability of finding a solute next to another solute and q is the probability of finding a solvent next to a solute. In our simulated alloy, p and q equal to the solutes and Al concentration, 1.44% and 98.56% respectively. There are 12 possible positions for solutes next to each other and all 18 positions next to a pair of solutes have to be occupied by solvent atoms, hence the numbers in Eq. (6). Eq. (7) can be justified in an analogous way. From equations (6) and (7), a number density of dimers and trimers of around 10^{26} m^{-3} can be derived for the random state, which agrees well with the numbers found in Fig. 2 for the initial stage.

Even after NA for an extensive period of time, e.g. t=1000 min, most of the clusters are still dimers and trimers. In the recent publication, Starink has successfully modelled the strength of Al-Cu-Mg alloys from the contribution of co-clusters [22], which appears reasonable since dimers and trimers are so abundant that they can play an important role.

The clustering kinetics in Al-Mg-Si alloys is very fast even at 'room temperature' [3,7,19]. Two stages of clustering have been be found within the first 100 min of NA in both PALS and in-situ resistivity measurements, giving rise to pronounced changes of the respective signal. A low temperature clustering process (called 'C1') can be observed in DSC experiments with linear heating rates in the temperature range of 20-80^{o}C. This process has an activation energy of ≈50 kJ/mol in an alloy with the same composition as in this simulation [23]. With this small activation energy, C1 can be easily activated at room temperature. From our simulation, a pronounced increase in the number density of clusters is found in the first 2 min of NA, which confirms that the kinetics of clustering in Al-Mg-Si is indeed fast. It is actually faster than the processes measured experimentally but one has to keep in mind that the conversion of Monte

Carlo time to real time using Eq.(3) relies on the vacancy density C_V. We do not know how many vacancies are lost during quenching and there could be a continuous loss of vacancies in a real system. This would stretch the time axis of the simulation.

The average jump frequency of the vacancy is about 2500 s^{-1} in our simulation. It is much higher than the vacancy jump frequency in pure aluminium, which is also simulated and is ~600 s^{-1}. The higher jump frequency in the alloy compared to pure Al is thought to be due to the presence of Si, which has a higher diffusion coefficient and lower activation energy for diffusion, see Table I. Together with the favourable interaction energy with vacancies, see Table II, this leads to faster kinetics of clustering.

From the evolution of number density and fraction of solute atoms in clusters, the clustering process seems to have some similarities with nucleation, growth and coarsening in a precipitation process. Therefore, the number density of clusters is plotted on a logarithmic scale as a function of logarithmic time in order to compare it with classical nucleation and coarsening processes. In continuous nucleation, the nucleation rate can be expressed as [24][25]

$$\dot{N}(T(t)) = N_0 \exp\left(-Q_N/RT(t)\right), \quad (8)$$

where N_0 is the temperature-independent nucleation rate, Q_N is the nucleation activation energy, R is the gas constant. From Eq. (8) it follows that for constant T, of the number of nuclei formed per unit time in a unit volume is constant, i.e. $N \propto t$ or $\log(N) \propto \log(t)$.

Figure 4a shows the fitting of this kind of relation to stage 1, i.e. for t < 2 min. From the number density, the value of the initial random cluster was subtracted and then fitted by a power law. We find that in stage 1, $N \propto t^{0.72}$. When compared to classical nucleation theory where $N \propto t$, it can be found that in stage 1 clustering is slower, but the difference is small.

In stage 2, growth of clusters is mainly by coalescence of clusters, while addition of solute still occurs. No classical growth theory can be found to describe this. In stage 3, the fraction of solute atoms in the clusters is saturated, indicating that the composition of the matrix has almost reached an equilibrium. Therefore, it is reasonable to verify whether the coarsening of clusters resembles Ostwald ripening. The relationship between number density and time in classical Ostwald ripening is given by Lifshitz, Wagner and Slyozov (LSW) [26] as $N \propto 1/r^3 \sim 1/t$, where a constant cluster volume is assumed. The same fitting procedure has been done for stage 3, see Fig. 4b. It is found that $N \propto t^{-0.08}$ and therefore the decrease of the number density indicates that the coarsening process in the simulation is much slower (~12.5 times) than predicted by LSW theory. Coarsening could be retarded by the attractive interaction between vacancies and both Mg and Si, see Table II. Vacancies are then trapped in the clusters most of the time, thus delaying the diffusion of solutes.

In our simulations, input parameters are taken from the literature, see Tables I and II. As these parameters vary, the question arises how robust the simulations are. A physical time t is assigned to each Monte Carlo step by using Eq.(3), which contains the vacancy concentration C_V, which in turn depends on the vacancy formation energy. The varying formation energies and entropies of vacancies provided by different sources [17,18] give rise to vacancy concentrations ranging from 3.6×10^{-5} to 2.7×10^{-4}. This range, according to Eq. (3), leads to a rescaling of physical time. Moreover, it can be found that the average vacancy jump frequency is about 2500 s^{-1} in our simulation. However, if other experimental or theoretical values for the diffusion activation energy of a vacancy are used [27,28,29], the vacancy jump frequency can be as high as 60000 s^{-1} or as low as 300 s^{-1}, leading to a pronounced rescaling of the physical

time appearing in Fig. 2, too.

Size and composition of clusters are strongly related to the interaction energies as they are used to calculate the vacancy jump frequency, see Eq. (2). Different vacancy and solute binding energies can be found and this would influence the simulation [30]. This can be illustrated by the example that the binding energy between a vacancy and a Mg atom has been reported to be both positive and negative in the literature. Compared with our assumption of attractive binding, based on Refs. 14,15,16, the opposite case (supported by Ref. 30) would make the diffusion of Mg more difficult, lower the content of Mg in clusters and result in smaller average cluster sizes. We avoid an eclectic and arbitrary choice of parameters by taking them from two well-documented sources only.

5. Conclusions

KMC simulations were performed to study the kinetics of clustering in Al-Mg-Si alloys using recently published input parameters. It is found that,

1. different stages are observed, namely: stage 1 with an increase of the number density of clusters, stage 2, during which clusters coarsen while still attracting solute atoms from the matrix, stage 3 where clusters coarsen and no more solute aggregates.
2. clustering is a fast process, with the most significant increase of number density taking place within 2 min, while the volume fraction of solute located in clusters occurs within the first 100 min,
3. The results from the model depend on the input parameters, and therefore the predictive power of the simulation depends on their reliability. With our choice of

parameters, the experimentally known situation is explained qualitatively, but comparison with experimental dada should not be taken to literally.

Acknowledgement

The authors would like to thank Dr. N. Lazarev for helpful discussions.

Corresponding address:

Zeqin Liang

Institute of Applied Materials, Helmholtz-Zentrum Berlin für Materialien und Energie, Hahn-Meitner-Platz 1, D-14109 Berlin, Germany

Tel.: +49 30 806242053

Fax: +49 30 806243059

E-mail: zeqin.liang@helmholtz-berlin.de

Figure and Table Captions

Figure 1: Simulated atom distributions at selected times in Al-0.67Mg-0.77Si alloy. Pink: Mg, blue:Si. (a) initial state, (b) t=1 min, (c) t=10 min, (d) t=100 min, (e) t=1000 min. Al atoms and isolated Mg/Si atoms are not shown.

Figure 2: Calculated cluster density and fraction of solutes in clusters as a function of natural ageing time.

Figure 3: Size distribution of clusters after different natural ageing times. (a) initial stage (b) t=1 min, (c) t=10 min, (d) t=100 min, (e) t=1000 min.

Figure 4: Fitting of power laws to the number densities of clusters in (a) stage 1, (b) stage 3.

Table I: Kinetic parameters used for the calculations (taken from Ref. 13).

Table II: interaction energies used for the calculations (taken from Refs. 14 and 15).

6. References

[1] J. Hirsch: Mater. Sci. Forum 242 (1997) 33

[2] I. Kovács, J. Lendvai and E. Nagy: Acta Metall. 20 (1972) 975

[3]J. Banhart, C.S.T. Chang, Z. Liang, N. Wanderka, M.D.H. Lay and A. J. Hill: Adv. Eng. Mater. 12 (2010) 559

[4] A. Serizawa, S. Hirosawa, and T. Sato: Metall. Mater. Trans. A 39 (2008) 243

[5] M. Torsæter, H.S. Hasting, W. Lefebvre, C.D. Marioara, J.C. Walmsley, S.J. Andersen and R. Holmestad: J. Appl. Phys 108, (2010) 0732527

[6] M. Murayama and K. Hono: Acta Mater. 47 (1999) 1537

[7] J. Banhart, M.D.H. Lay, C.S.T. Chang, and A.J. Hill: Phys. Rev. B. 83 (2011) 014101

[8] E. Clouet, C. Hin, D. Gendt, M. Nastar and F. Soisson: Adv. Eng. Mater. 8 (2006) 1210

[9] E. Clouet, M. Nastor and C. Sigli: Phys. Rev. B 69 (2004) 064109

[10] S. Hirosawa, T. Sato, A. Kamio, HM. Flower: Acta Mater. 48 (2000) 1797

[11] G. Sha, A. Cerezo: Acta Mater.53 (2005) 907

[12] S. Müller, L.-W. Wang and A. Zunger: Modell. Simul. Mater. Sci. Eng. 10 (2002) 131

[13] M. Mantina, Y. Yang, L.Q. Chen, Z.K. Liu, C. Wolverton: Acta Mater. 57 (2009) 4102

[14] S. Hirosawa, F. Nakamura, T. Sato: Mater. Sci. Forum, 283 (2007) 561-565

[15] T. Hoshino, R. Zeller and P.H. Dederichs: Phys. Rev. B 53 (1996) 2216

[16] S. Hirosawa, F. Nakamura, T. Sato and T. Hoshino: J.JILM, 56 (2006) 621

[17] K.M. Carling, G. Wahnström, T.R. Mattsson, N. Sandberg and G. Grimvall: Phys. Rev. B. 67 (2003) 054101

[18] P. Erhart, P. Jung, H. Schult, and H. Ullmaier, in Atomic Defects in Metals, Berlin, Springer-Verlag (1991)

[19] C.S.T. Chang, J. Banhart: Metall. Mater. Trans. A 42 (2011) 1960

[20] K. Momma and F. Izumi: J. Appl. Crystallogr. 41 (2008) 653

[21] L.T. Stephenson, M.P. Moody and S.P. Rigner: Philos. Mag. 91 (2011) 17, 2200

[22] M.J. Starink and S.C. Wang: Acta Mater. 57 (2009) 2376-2389

[23] C.S.T. Chang, Z. Liang, E. Schmidt, and J. Banhart: submitted to Int. J. Mater. Res.

[24] J.W. Christian: The theory of transformation in metals and alloys, Oxford, Pergamon Press (2002)

[25] E.J. Mittemeijer and F. Sommer: Z. Metallkde., 93 (2002), 5

[26] R.W. Cahn: Physical Metallurgy, Amesterdam, North-Holland Physics Publishing (1983)

[27]J.B. Adams: J. Mater. Res. 4 (1989) 102.

[28] S. Fujikawa, K. Hirano: Mater. Sci. Eng. 27 (1977) 25

[29] Y. Du, Y.A. Chang, B. Huang, W. Gong, Z. Jin, H. Xu, Z. Yuan, Y. Liu, Y. He, F. Y. Xie: Mater. Sci. Eng. A (2003) 140

[30] C. Wolverton: Acta Mater. 55 (2007) 5867

Figures

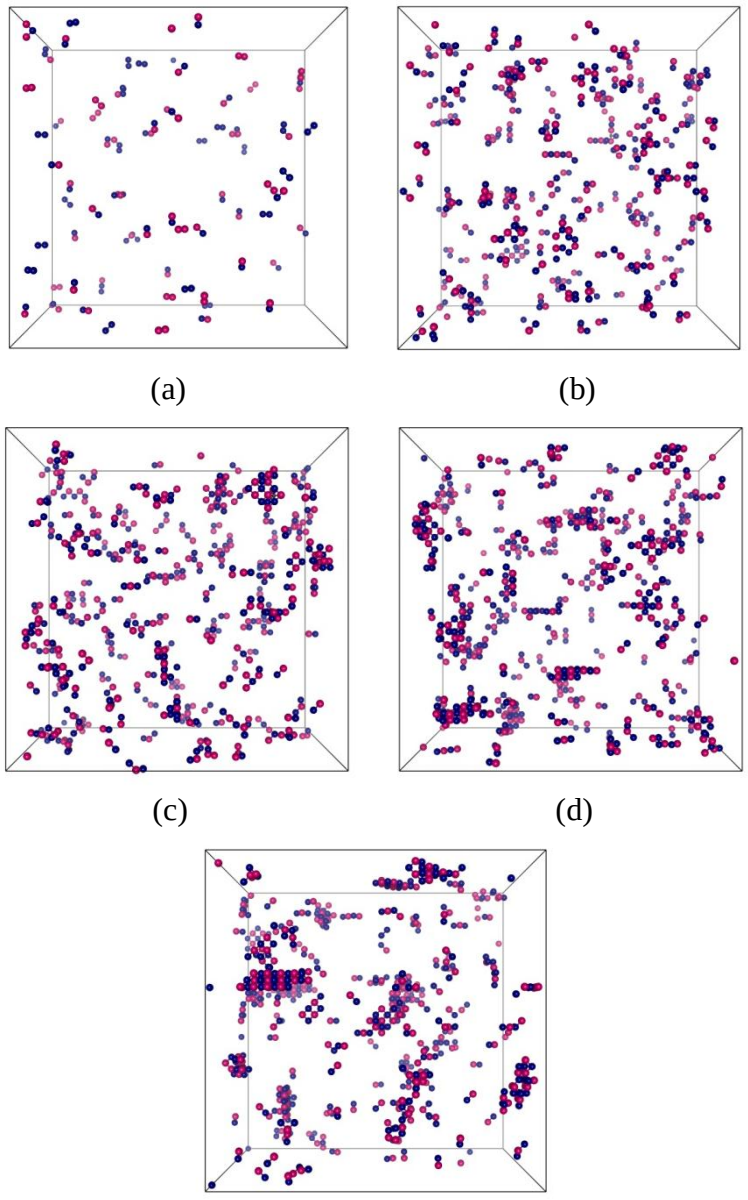

Figure 1: Simulated atom distributions at selected times in Al-0.67Mg-0.77Si alloy. Pink: Mg, blue:Si. (a) initial state, (b) t=1 min, (c) t=10 min, (d) t=100 min, (e) t=1000 min. Al atoms and isolated Mg/Si atoms are not shown.

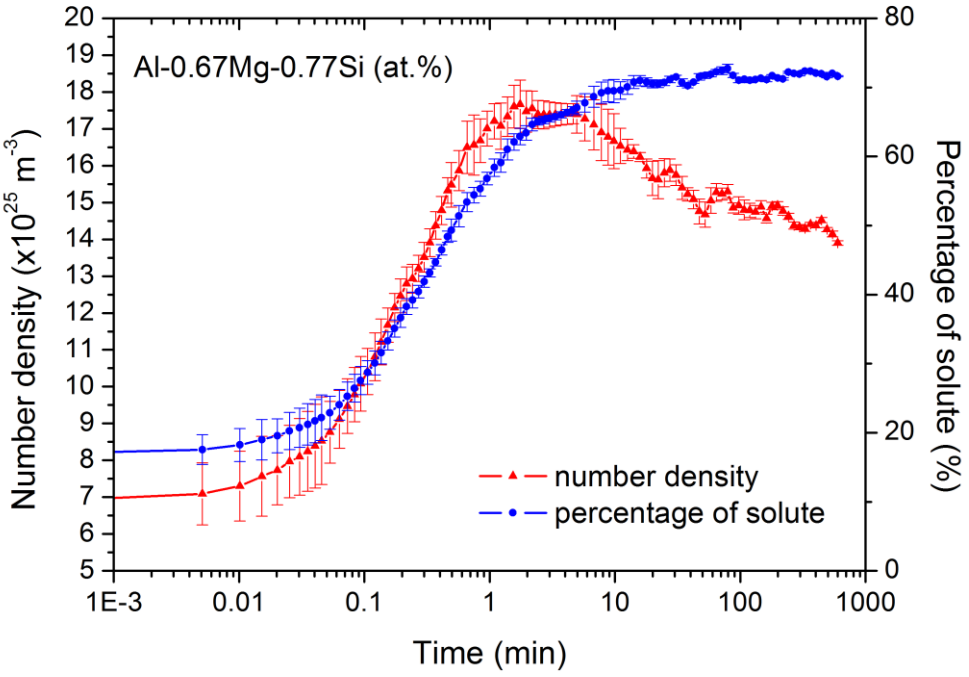

Figure 2: Calculated cluster density and fraction of solutes in clusters as a function of natural ageing time.

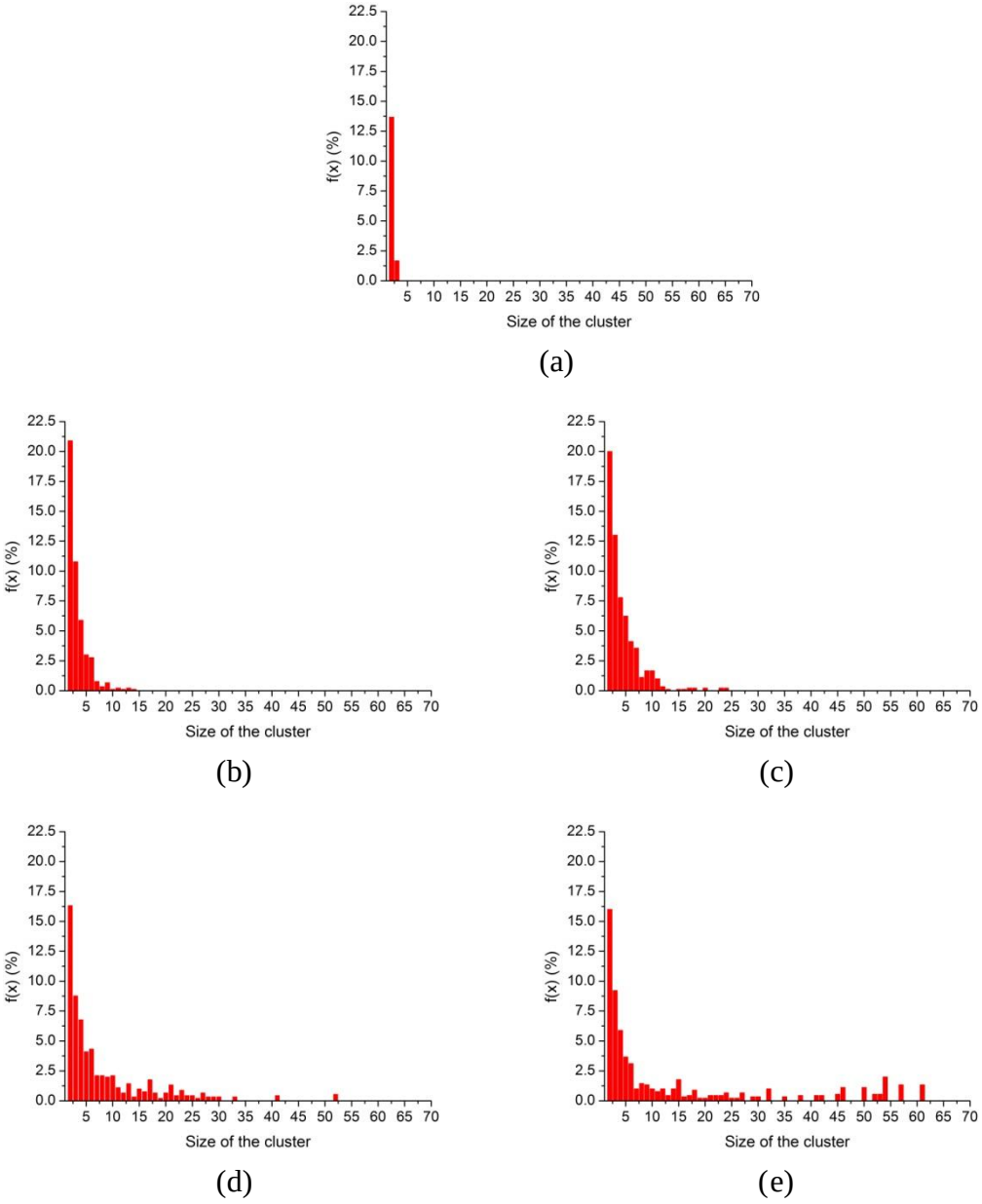

Figure 3: Size distribution of clusters after different natural ageing times. (a) initial stage (b) t=1 min, (c) t=10 min, (d) t=100 min, (e) t=1000 min.

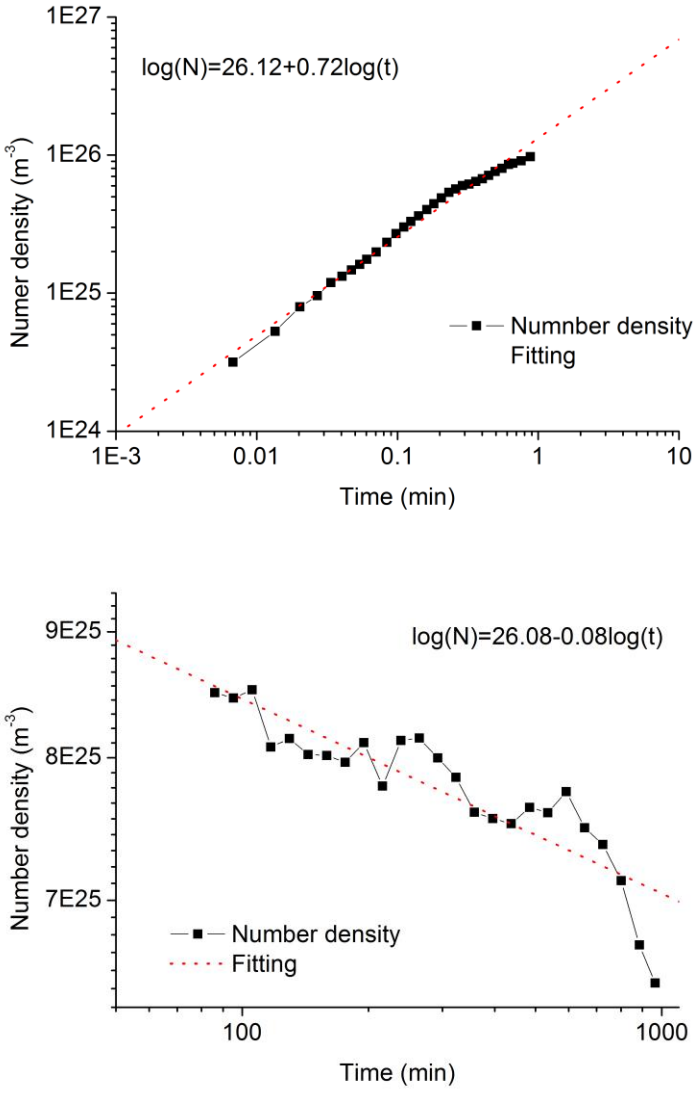

Figure 4: Fitting of power laws to the number densities of clusters in (a) stage 1, (b) stage 3.

Table

Tables

Table I Kinetic parameters taken from Ref. 13

ν_{Al}	1.66×10^{13} /s
ν_{Mg}	1.86×10^{13} /s
ν_{Si}	1.57×10^{13} /s
E_{Al}^{d}	1.29eV
E_{Mg}^{d}	1.27eV
E_{Si}^{d}	1.15eV
E_{V}^{f}	0.63eV

Table II Chemical interaction energies (eV +favored -repulsive) taken from Refs 14, 15

ε_{Al-V}	0
ε_{Mg-V}	+0.015
ε_{Si-V}	+0.025
ε_{Al-Al}	0
ε_{Al-Si}	0
ε_{Al-Mg}	0
ε_{Mg-Si}	+0.04
ε_{Mg-Mg}	-0.04
ε_{Si-Si}	-0.03